Effects of Plastic Anisotropy and Yield Surface Shape on Sheet Metal Stretchability

K. S. CHAN

The influence of plastic anisotropy and the shape of the yield surface on localized necking of thin metal sheets is examined. Forming limit curves (FLCs) of strain hardening, rate-sensitive sheets including Ti alloys, Al alloys, and steels are calculated on the basis of the Marciniak-Kuczynski approach using the quadratic Hill or the Drucker yield function in conjunction with either the flow or deformation theory of plasticity. The roles of the R-value and the yield surface shape in biaxial stretchability of sheet metals are delineated and discussed in relation to the plasticity theories and yield functions. It is concluded that the limit strains decrease with increasing R-value in the $\varepsilon_2 > 0$ region of an FLC but increase with the R-value in the $\varepsilon_2 < 0$ region, and are independent of the R-value at plane strain conditions. These mixed, strain-path dependent effects are explained in terms of the shape of the yield surface and a recently proposed critical thickness strain criterion.

I. INTRODUCTION

SHEET metals subjected to biaxial stretching usually fail by localized necking. Hence, the stretchability of sheet metals depends on the material's resistance to localized necking and, in particular, upon material factors which delay the onset of such a plastic instability. The beneficial effects of strain hardening and strain rate hardening on stretchability are well known; both of these effects increase the forming limit strains of sheet metals, which are usually defined in terms of the maximum principal strains (ε_1 and ε_2) attainable from sheets prior to the onset of localized necking.[1,2] It is well known that a high degree of plastic anisotropy as represented by a large R-value, which is the ratio of width strain to thickness strain in a uniaxial tensile specimen, promotes formability in drawing. Recent stretch forming studies on strongly textured Ti-alloy sheets indicate that a large R-value also increases the resistance to localized necking in stretching conditions involving negative minor strains.[3,4] The experimental results,[3,4] a theoretical analysis[5] which assumes localized necking being initiated from an imperfection aligned along Hill's direction of zero-extension[6] and a reexamination[5] of Hill's theory,[6] all indicate that in the $\varepsilon_2 < 0$ regime, the enhancement of the forming limit strains by the R-value can be understood in terms of a critical thickness strain criterion for localized necking. According to this criterion, ε_1^* increases with the R-value as the result of increasing difficulties in attaining a critical thickness strain (ε_3^*) at a higher R-value.

The effects of the R-value on biaxial stretching involving positive minor strains, on the other hand, remain inconclusive because of difficulties in separating the effects of plastic anisotropy from those of strain hardening and strain rate hardening in sheets with relatively similar, low R-values[1] ($R < 2$) and of difficulties in determining whether localized necking takes place prior to fracture in sheets with high R-values.[4] Theoretical efforts to elucidate the effects of the R-value are complicated by the fact that the calculated FLCs, in addition to strain hardening and strain-rate hardening, also depend on the choice of the yield function[7,8] (for example, quadratic *vs* nonquadratic Hill yield functions), the plasticity theory[9,10,11] (flow *vs* deformation or vertex theories of plasticity), and on whether localized necking originates from material imperfections,[12] instability resulting from the presence of a vertex on the yield surface,[9] or void growth.[13] Since Hill's direction of zero-extension[6] does not exist when $\varepsilon_2 > 0$, neither Hill's theory nor the critical thickness strain criterion for localized necking is applicable under these biaxial stretching conditions.

The hypothesis that localized necking initiates from material imperfection was first proposed by Marciniak and Kuczynski[12] (M-K), with later extensions by Sowerby and Duncan,[14] Hutchinson and co-workers,[6,8,11] as a means of describing localized necking in biaxial stretching when ε_2 is positive. The M-K analysis assumes the presence of a material imperfection in the form of a linear groove which lies parallel to the ε_2 direction. Imposing the same ε_2 inside and outside the groove while proportional straining is maintained outside the groove, M-K have shown that deformation within the groove occurs at a faster rate than the rest of the sheet. The concentration of strain within the groove eventually leads to the plane strain condition ($d\varepsilon_2 = 0$) within the groove and to localized necking. Using flow theory of plasticity in conjunction with Hill's quadratic yield function,[15] Marciniak, Kuczynski, and Pokora[16] and also Sowerby and Duncan[14] have demonstrated that by virtue of the sharp curvature in the smooth yield surface, a high R-value material containing an imperfection and stretched under equi-biaxial tension would locally attain the plane strain condition for localized necking at an earlier stage of the straining process and result in lower forming limit strains than that of a low R-value material. Similar dependence of forming limit strains on the R-value are also observed in theoretical FLC calculations[7,8] which are based on the flow theory and the nonquadratic Hill[17] or the Bassani yield function.*[18]

*The Bassani yield function is: $|\sigma_1 + \sigma_2|^N + N/M(1 + 2R)\sigma_u^{N-M}|\sigma_1 - \sigma_2|^M = [1 + N/M(1 + 2R)]\,\sigma_u^N$, where σ_u is the yield stress in uniaxial tension, and N and M are constants greater than or equal to 1. For $N = M$, the Bassani yield function reduces to the non-quadratic Hill yield function.

That localized necking can originate from instability in the form of a vertex on the yield surface was first recognized

K. S. CHAN is Research Engineer, Department of Materials Sciences, Southwest Research Institute, 6220 Culebra Road, P.O. Drawer 28510, San Antonio, TX, 78284.

Manuscript submitted March 13, 1984.

by Storen and Rice[9] and later by Hutchinson and Neale,[10] and by Neale and Chater.[7] Based on the rationale that the deformation theory of plasticity is equivalent to a flow theory which permits the development of a pointed vertex on the yield surface, these authors incorporated deformation theories of plasticity into classical bifurcation analyses demonstrating that for rate-insensitive materials localized necking can occur as the result of the development of a sufficiently sharp vertex on the yield surface during plastic straining such that the plane strain condition for localized necking is satisfied. The vertex theory was subsequently extended to imperfect, rate-sensitive materials by incorporating deformation theories of plasticity into the M-K analysis.[7,10] Comparisons of these calculations with results obtained based on the flow theory with smooth yield surface indicate that the computed limit strains are sensitive to whether or not a pointed vertex is allowed to develop on the yield surface; consequently, the shape of the yield surface and the choice of plasticity theories in FLC calculation are important. In particular, the work of Neale and Chater[7] reveals that the role of the R-value in biaxial stretching appears to be relatively small when the FLC predictions based on deformation theory are compared to those predicted by the flow theory with smooth yield surfaces.

The objective of this paper is to delineate the roles of plastic anisotropy and the shape of the yield surface in localized necking of sheet metals under biaxial stretching ($\varepsilon_2 > 0$). Theoretical FLC calculations will be performed on the basis of the M-K analysis and using the quadratic Hill yield function in conjunction with either the flow or deformation theories of plasticity. The calculated FLCs will be compared with the experimental curves of a variety of sheet metals which exhibit a wide range of R-values and include a number of Ti alloys, Al alloys, and steels. In light of recent experimental data[19] which indicate that the biaxial response of HY80 steel is better described by the Drucker yield function,[20] the constitutive aspects of FLC calculations will also be examined. The assessment will focus on steels and compare experimental data with theoretical results based on the flow and deformation theories of plasticity, including one which incorporates the Drucker yield function. Although this study is mainly concerned with the $\varepsilon_2 > 0$ side of the FLC, results for the case of $\varepsilon_2 < 0$ are also presented for the sake of completeness. The present effort thus augments recent work by Chan, Koss, and Ghosh[5] who examined, among other material factors, the effects of the R-value on localized necking at negative minor strains, and previous studies on the effects of strain hardening and strain rate hardening on sheet metal stretchability by Ghosh,[2] Lee and Zaverl,[21] and Thomas, Oh, and Gegel.[22]

II. M-K ANALYSIS FOR IMPERFECT SHEETS

The procedures adapted in the present study for computing the $\varepsilon_2 > 0$ regime of an FLC follow closely the analyses of Marciniak, Kuczynski, and Pokora[16] and those of Hutchinson and Neale,[10] Neale and Chater[7] for the cases where the methods of analysis are based on the flow and deformation theories of plasticity, respectively. For the $\varepsilon_2 < 0$ region, the analysis of Chan, Koss, and Ghosh[5] is used. Since the mathematical details of the analyses are well documented, they will not be repeated here; only the essentials are outlined below.

A. *Constitutive Relations*

The sheet metals are assumed to exhibit isotropic hardening and a power law type effective stress-effective strain constitutive relation:

$$\bar{\sigma} = K\bar{\varepsilon}^n\dot{\bar{\varepsilon}}^m \qquad [1]$$

where $\bar{\sigma}$ = effective stress, $\bar{\varepsilon}$ = effective strain, n = strain-hardening exponent, K = strength constant, $\dot{\bar{\varepsilon}}$ = effective strain rate, and m = strain-rate sensitivity exponent. While use of Eq. [1] is common and that it appears to be adequate for the materials considered here, it should be recognized that neither it nor any multiplicative power law constitutive equation is able to predict the dependence of an FLC on the absolute strain rate unless the material constants themselves are a function of strain rate.[22] It should also be noted that Eq. [1] is identical to the Swift equation[23] if a pre-strain term is added to $\bar{\varepsilon}$. Since the pre-strain term is generally small (<0.01), the material parameters in Eq. [1] which substantially affect the limit strain calculations are the n and m values.

B. *Yield Functions and the Associated Flow Laws*

The quadratic Hill yield function is frequently used to describe the biaxial behavior of the thin sheets. For this yield criterion, assuming normal anisotropy, the effective stress and effective strain for plane stress ($\sigma_3 = 0$) are given by[15] (see Appendix I)

$$\sigma = \sqrt{\frac{3}{2}}\sqrt{\frac{R+1}{R+2}}\left[1 - \frac{2R}{1+R}\alpha + \alpha^2\right]^{1/2}\sigma_1 \qquad [2]$$

$$d\bar{\varepsilon} = \sqrt{\frac{2}{3}}\sqrt{\frac{(2+R)(1+R)}{1+2R}} \cdot\left[1 + \frac{2R}{1+R}\rho + \rho^2\right]^{1/2} d\varepsilon_1 \qquad [3a]$$

where

$$\alpha = \frac{\sigma_2}{\sigma_1} \qquad [3b]$$

$$\rho = \frac{d\varepsilon_2}{d\varepsilon_1} \qquad [3c]$$

According to the flow theory of plasticity, the associated flow laws are

$$\frac{d\varepsilon_1}{a\sigma_1 - \sigma_2} = \frac{d\varepsilon_2}{a\sigma_2 - \sigma_1} = \frac{d\varepsilon_3}{(1-a)(\sigma_1 + \sigma_2)} = \frac{3R\,d\bar{\varepsilon}}{2(2+R)\bar{\sigma}} \qquad [4]$$

where $a = (1 + R)/R$. It can be shown from Eq. [4] that α is related to ρ, and

$$\rho = \frac{a\alpha - 1}{a - \alpha} \qquad [5]$$

On the other hand, the corresponding deformation theory relations are obtained by replacing $d\varepsilon_i$ and $d\bar{\varepsilon}$ in Eqs. [3] and [4] by their total values ε_i and $\bar{\varepsilon}$ ($i = 1, 2$, or 3). It should be noted that the deformation theory is identical to the flow theory for simple, proportional loadings. For continued plastic flow with small deviations from proportional

loading such as that experienced in an imperfection, the deformation theory yields plastic strain increments which are not normal to the smooth, quadratic yield surface. However, the use of the deformation theory in these loading paths can be rationalized on the basis that the yield surface develops a pointed vertex during plastic straining.[9] At such a vertex, the plastic strain increment vector can lie anywhere between the two outward normals of the yield vertex.

The Drucker yield function, g, which contains both the J_2 (the second deviatoric stress invariant) and J_3 (the third deviatoric stress invariant) terms is applicable for sheets with $R = 1$ and can be represented by[19]

$$g = \frac{27}{27 - 4C}[J_2^3 - CJ_3^2] \qquad [6]$$

where C is a constant. Based on Eq. [6], the effective stress for plane stress ($\sigma_3 = 0$) is

$$\bar{\sigma}_D = [1 - \alpha + \alpha^2]^{1/2}\left[\frac{27}{27 - 4C}(1 - CJ_3^2/J_2^3)\right]^{1/6}\sigma_1 \qquad [7]$$

with $J_2 = b\sigma_1^2$
$J_3 = h\sigma_1^3$
$b = [1 - \alpha + \alpha^2]/3$
$h = -(2 - \alpha)(2\alpha - 1)(1 + \alpha)/27$

and the corresponding incremental effective strain is obtained from Eq. [3] by substituting $R = 1$. The incremental plastic strain components are obtained from the associated flow rules (see Appendix I), and the plastic strain ratio ρ is obtained as follows:[19]

$$\rho = \frac{9(2\alpha - 1)b^2 - 2C(2\alpha^2 - 2\alpha - 1)h}{9(2 - \alpha)b^2 - 2C(2 - 2\alpha - \alpha^2)h} \qquad [8]$$

Plastic volume constancy is assumed such that

$$d\varepsilon_1 + d\varepsilon_2 + d\varepsilon_2 = 0 \qquad [9]$$

The constant C in the Drucker theory is a fitting parameter which determines the relative contributions of J_2 and J_3 in the yield function. For $C = 0$, the contribution of J_3 is zero, and the Drucker yield surface is reduced to the von Mises, the quadratic Hill (with $R = 1$) and, for bcc metals, the pencile-glide yield surfaces.[24] A finite, positive C-value affects the shape of the yield surface and consequently the plastic strain ratio at a given stress state. Chan, Lindholm, and Wise[19] recently noted that in the range of $C = 1.75$ to 2.25, the Drucker yield surface is practically identical to the Bishop-Hill yield surface[25] calculated by Bassani[18] for isotropic bcc polycrystalline metals deforming by $\{110\}\langle 1\bar{1}1\rangle$ slip. Both the Bishop-Hill and the Drucker yield surfaces were confirmed for a HY80 steel[19] and less conclusively for a HY100 steel.[26] Thus, upon a proper choice of the C-value, the Drucker yield function can be used as an analytical expression for either the pencile-glide or the Bishop-Hill $\{110\}\langle 1\bar{1}1\rangle$ yield surfaces. A comparison of the Drucker yield surface with the quadratic and the nonquadratic yield surfaces for the case of $C = 2.25$, $R = 1$, and $M = 1.6$ in the appropriate theories is shown in Figure 1(a). Compared to the quadratic Hill yield surface (which is identical to the von Mises yield surface when $R = 1$), the Drucker yield surface exhibits a shape curvature near the equibiaxial tension ($\sigma_1 = \sigma_2$) region and a rather extended region where the plane strain condition ($\rho = 0$) is approximately satisfied, as illustrated in Figure 1(b) which shows the plastic strain ratio as a function of the stress ratio, α. On the other hand, the nonquadratic Hill yield surface is seen to elongate in the $\sigma_1 = \sigma_2$ direction and the plane condition is satisfied at $\alpha = 0.75$ (see Figure 1(a)).[27]

C. *M-K Approach*

The M-K approach postulates that a linear material imperfection exists on the plane of a sheet metal deforming under biaxial stresses σ_1 and σ_2. The orientation of the imperfection is taken to lie perpendicular to the σ_1 axis in the original M-K analysis for biaxial stretching involving positive minor strains ($\varepsilon_2 > 0$) (Figure 2(a)) but has been modified to lie in the direction of zero-extension for strain states involving negative minor strains ($\varepsilon_2 < 0$) (Figure 2(b)). As shown in Figure 2, the imperfection is designated as region B, and its initial thickness is t_{oB}. The region outside the imperfection is considered to be uniform and is referred to region A; its initial thickness is designated as t_{oA}.

The governing equations in the M-K analysis are the load equilibrium and compatibility conditions between regions A and B. For sheets with perpendicular imperfection and under biaxial stretching ($\varepsilon_2 > 0$), the equilibrium equation is:[16]

$$t_A\sigma_{1A} = t_B\sigma_{1B} \qquad [10]$$

or

$$(\sigma_{1A}/\bar{\sigma}_A)(\bar{\varepsilon}_A)^n\dot{\bar{\varepsilon}}_A^m \exp(\varepsilon_{3A}) = f(\sigma_{1B}/\bar{\sigma}_B)(\bar{\varepsilon}_B)^n\dot{\bar{\varepsilon}}_B^m \exp(\varepsilon_{3B}) \qquad [11]$$

where t is the thickness of the sheet, ε_3 is the thickness strain, f is the imperfection factor which is defined as $(K_B t_{oB})/(K_A t_{oA})$, and the quantities $(\ )_A$ and $(\ )_B$ represent the quantities in regions A and B, respectively. For a perpendicular imperfection, the corresponding compatibility equation between regions A and B is

$$d\varepsilon_{2A} = d\varepsilon_{2B} \qquad [12]$$

The limit effective strain $\bar{\varepsilon}_A$ for a specific constant plastic strain ratio in region A (ρ_A) can be obtained numerically by incremental solution of Eqs. [11] and [12] using the procedures described in Appendix II. For both flow and deformation theories, the incremental solution procedures are carried out until $d\bar{\varepsilon}_A$ is less than 1×10^{-4}. The limit strain components (ε_1^* and ε_2^*) are then calculated from $\bar{\varepsilon}_A$ using Eqs. [3] through [5].

D. *Critical Thickness Strain Criterion*

Using both the Hill theory[6] and an M-K analysis in which the imperfection is modified to lie at Hill's angle of zero-extension, Chan, Koss, and Ghosh[5] have demonstrated that in the strain states between uniaxial tension and plane strain, localized necking of sheet obeys a critical thickness strain criterion whether or not an imperfection is present; the criterion is represented by

$$\varepsilon_1^*(1 + \rho) = -\varepsilon_3^* = \text{constant} \qquad [13]$$

where ε_3^*, the critical thickness strain for localized necking, is equal to the n-value for rate-insensitive sheets without an

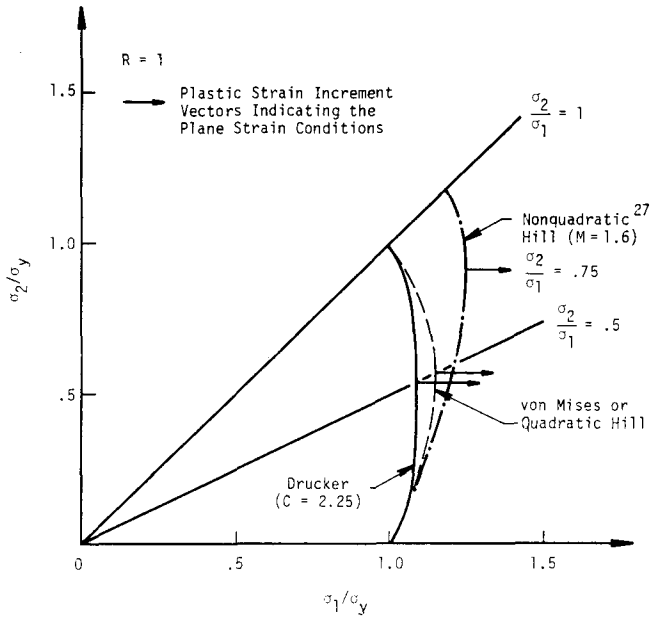

(*a*)

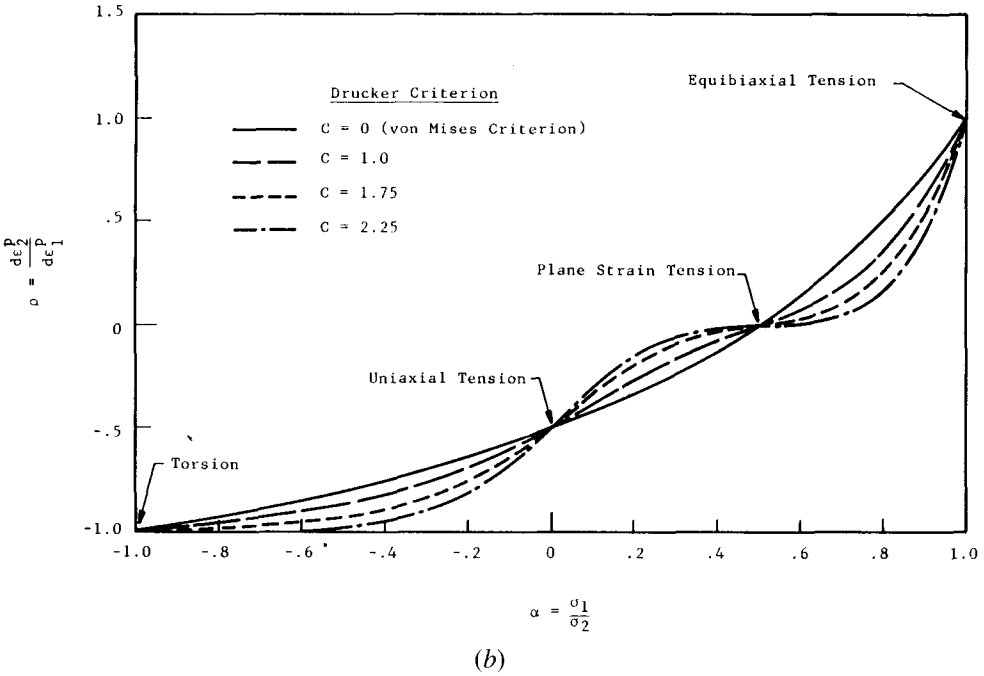

(*b*)

Fig. 1—(*a*) A comparison of the quadratic Hill yield function with the nonquadratic Hill and the Drucker yield functions for the case of $R = 1$. (*b*) A comparison of the plastic strain ratios for the Drucker yield function at various C-values. At $C = 0$, the Drucker yield function is reduced to the von Mises, quadratic Hill, and the pencile-glide yield functions.

imperfection but depends on the n, m, and f values for rate-sensitive, imperfect sheets. For imperfect sheets deformed under the plane strain condition, the magnitude of ε_3^* is equal to ε_1^* and can be obtained using the M-K analysis. The $\varepsilon_2 \leq 0$ side of the FLC can then be calculated using [13] and [3c].

III. RESULTS

A summary of the material parameters used in the FLC calculations is shown in Table I. The calculations are generally based on small imperfections ($f \geq 0.99$). Figure 3 compares the experimental FLC of a low R-value ($R = 0.77$) 2036-T4 sheet[1] with the calculated curves based on either flow theory or deformation theory. In the $\varepsilon_2 > 0$ region, deformation theory predicts limit strains which are in reasonable agreement with the experimental data, while flow theory tends to overpredict the limit strains. Additional results which compare the deformation theory predictions with the experimental FLCs are shown in Figure 4 for a number of aluminum alloys (6061-T4 Al,[1] 1100-H12 Al,[28] 5180-Al[29]) and in Figure 5 for a HSLA steel[30] (HS-4) and a

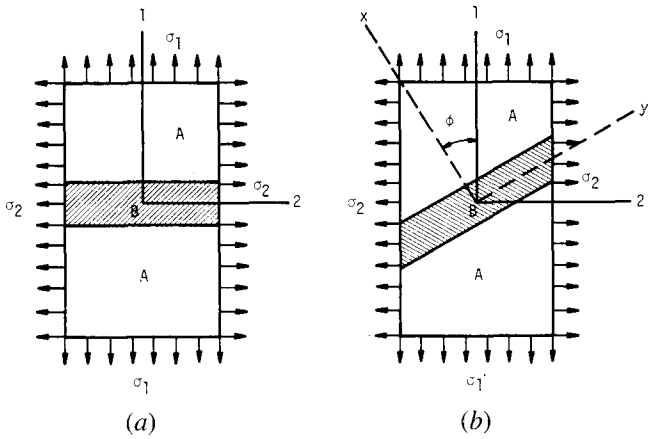

Fig. 2—A schematic view of a sheet containing a linear imperfection and subjected to the biaxial stresses σ_1 and σ_2. The orientation of the imperfection is: (*a*) normal to the σ_1 axis, (*b*) aligned at Hill's angle of direction of zero-extension, ϕ.

Table I. A Summary of the *n*, *m*, and *R* Values of Various Thin Metal Sheets

Material	*n*	*m*	*R*
1100-H12 aluminum[28]	0.04	0.003	0.76
2036-T4 aluminum[1]	0.24	0	0.77
5180-0 aluminum[29]	0.33	0	0.89
6061-T4 aluminum[1]	0.22	0	0.64
HSLA steel (HS4)[30]	0.16	0.005	0.80
A-K steel[33]	0.24	0.012	1.5
Low-carbon steels[1]	0.24	0.012	1.0
Ti-6Al-4V (weak texture, 24 °C)[31]	0.065	0.016	1.0
Ti-6Al-4V (weak texture, 538 °C)[31]	0.018	0.020	1.0
Ti-6Al-4V (basal texture)[4]	0.052	0.016	12.0
Ti-5Al-2.5Sn (basal texture)[4]	0.066	0.014	12.0
CP-Ti[32]	0.136	0.023	3.7

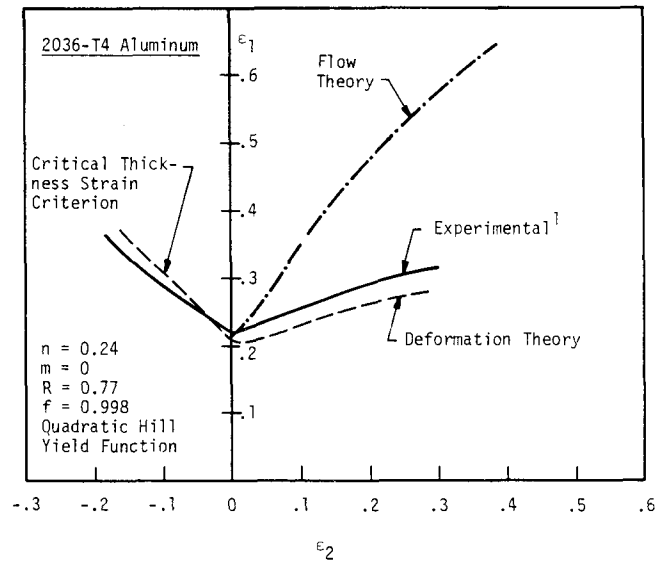

Fig. 3—Calculated and experimental FLCs of 2036-T4 aluminum.

Ti-6Al-4V alloy[31] with a weak texture and low R-value ($R = 1.0$). Figures 3 through 5 indicate that for these sheet metals with an R-value less than or equal to unity, deformation theory gives FLC predictions in the $\varepsilon_2 > 0$ region which are at least in fair agreement with the experimental data. In the $\varepsilon_2 < 0$ regime, the critical thickness strain criterion of Chan *et al.*[5] also gives results which are in good agreement with the experimental curves.

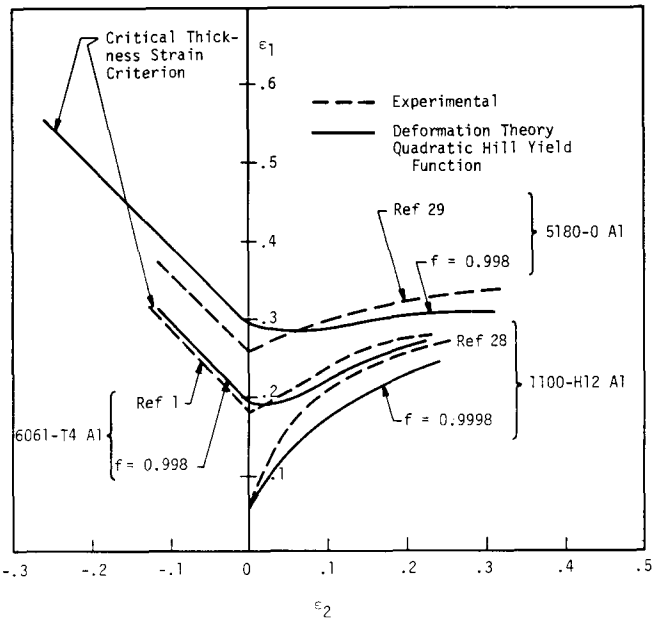

Fig. 4—Calculated and experimental FLCs of 1100-H12 Al, 5180-0 Al, and 6061-T4 Al.

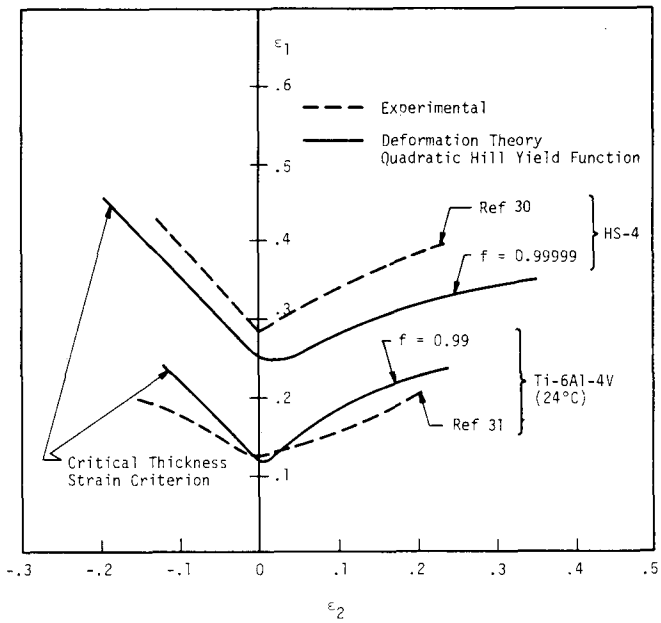

Fig. 5—Calculated and experimental FLCs of a HSLA steel (HS-4) and a weak-textured Ti-6Al-4V.

The results in Figure 6 indicate that for CP-Ti with a moderate R-value ($R = 3.7$) flow theory predicts limit strains which are in good agreement with the experimental data.[32] On the other hand, deformation theory is seen to underestimate the limit strains. For strongly textured Ti-6Al-4V and Ti-5Al-2.5 Sn sheets with $R = 12$, the flow theory predicts equi-biaxial limit strains ($\varepsilon_1^* = \varepsilon_2^* = 0.057$)

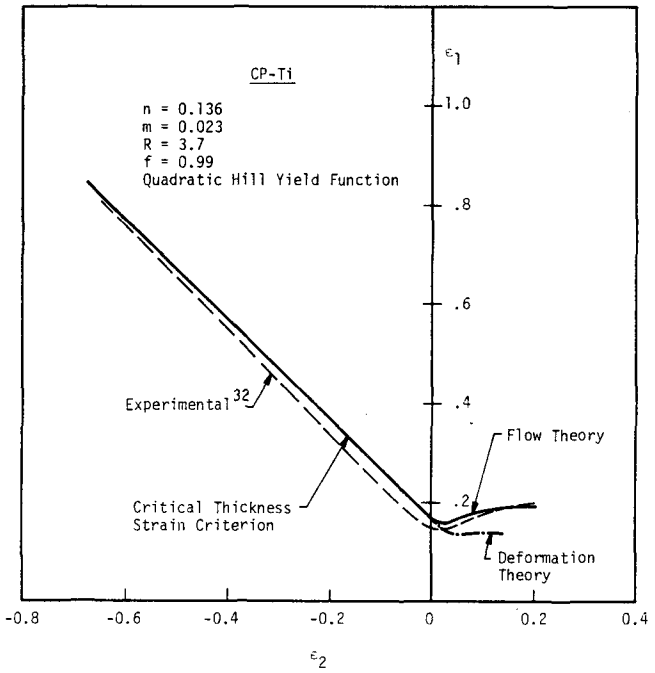

Fig. 6—Calculated and experimental FLCs of CP-Ti.

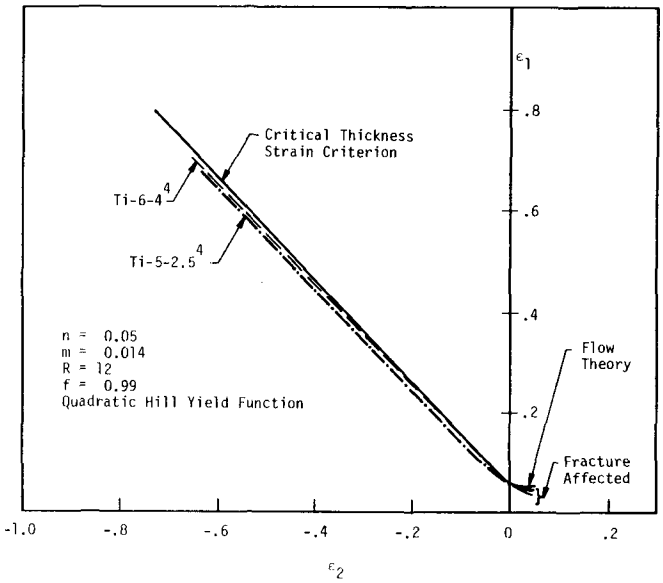

Fig. 7—Calculated and experimental FLCs of strongly textured Ti-6Al-4V and Ti-5Al-2.5Sn.

which are considerably smaller than those at uniaxial tension ($\varepsilon_1^* = 0.80$, $\varepsilon_2^* = -0.72$), as shown in Figure 7. The agreement between the experimental[4] and calculated FLCs is good in the $\varepsilon_2 < 0$ region but is inconclusive in the $\varepsilon_2 > 0$ region due to complications arising from intervention by fracture prior to localized necking.

Neither flow theory nor deformation theory yields satisfactory forming limit strains in the $\varepsilon_2 > 0$ region for A-K steel[33] when used with the quadratic Hill yield function. As seen in Figure 8, deformation theory tends to underestimate while flow theory tends to overpredict the limit strains, unless the flow theory results are modified by a fracture criterion as done by Ghosh.[2] A possible way for rectifying

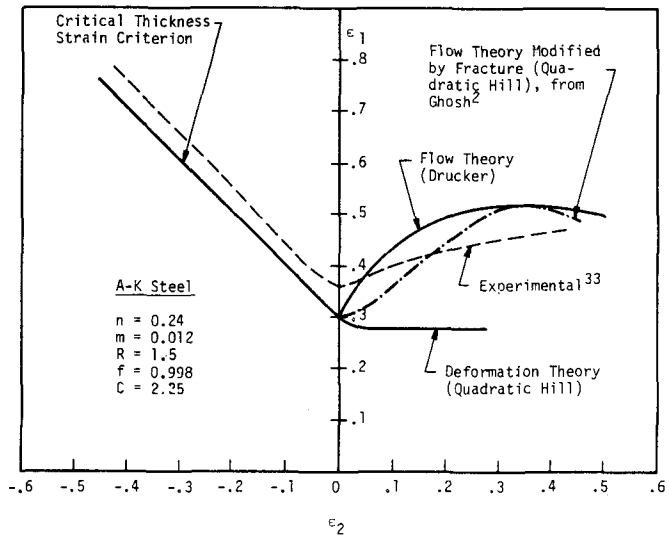

Fig. 8—Calculated and experimental FLCs of A-K steel. The FLC which is based on flow theory and modified by fracture is from Ghosh.[2]

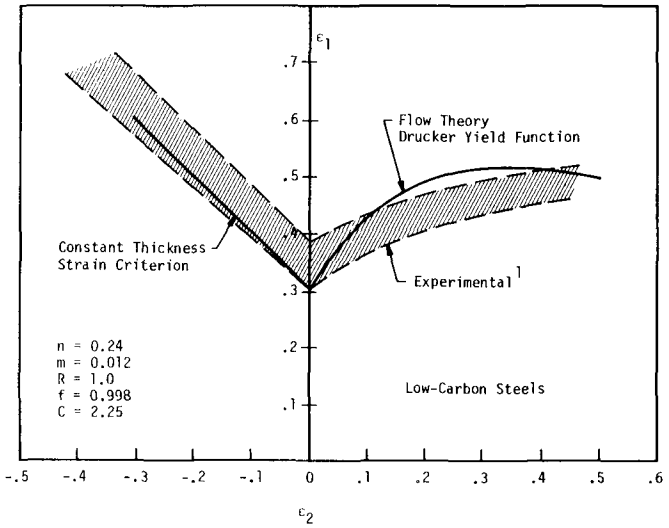

Fig. 9—Calculated and experimental FLCs of low-carbon steels.

the overprediction by the flow theory is by using the Drucker yield function instead of the quadratic Hill yield function, as demonstrated in Figure 8. Figure 9 shows that the FLC calculated based on the Drucker theory compares favorably with the forming limit scatter band of low-carbon steels.[1] In the $\varepsilon_2 < 0$ region, the critical thickness strain criterion again gives good agreement with the experimental data.

IV. DISCUSSION

In previous studies, Hutchinson and Neale have shown that theoretical FLCs calculated on the basis of the M-K approach depend critically on whether the flow or the deformation theory of plasticity is used.[10] Their calculations indicate that the deformation theory tends to give FLC results which are less sensitive to the size of the imperfection and the resulting forming limit strains are smaller than those

obtained based on the flow theory. Similar differences between the flow and the deformation theories were also observed in FLC results computed based on the Bassani yield function.[7] The present results not only confirm that the theoretical FLCs depend on the method of solution of Eqs. [11] and [12] but also demonstrate that neither the flow nor the deformation theory can predict with confidence the stretchability of a variety of sheet alloys (see Figures 3, 4, and 8). Thus, a judicious choice of plasticity theory is required for theoretical analysis of sheet metal formability.

None of the yield functions considered can predict the FLCs of sheet alloys exhibiting a wide range of R-values. Consequently, the yield function must also be selected judiciously. As demonstrated by Marciniak, Kuczynski, and Pokora,[16] and by Sowerby and Duncan,[14] one of the most important factors affecting the limit strain calculation using flow theory in the biaxial tension region is the shape of the yield locus. Specifically, the sharp curvature in the quadratic Hill's yield locus of a high R-value material containing an imperfection would allow the plane strain condition for localized necking to be attained at an earlier stage of deformation and result in reduced limit strains in the $\varepsilon_2 > 0$ region than that for a low R-value material. The good agreement between flow theory and experiment in Figure 6 for a moderately high R-value CP Ti appears to support these analyses. The use of the quadratic Hill yield function for CP-Ti is supported by the work of Lentz *et al.*[34] On the other hand, the large limit strains predicted by these analyses for the low R-value sheets ($R < 1$) are not realized. The discrepancy between theory (flow theory with quadratic Hill's yield function) and experiment observed in the low R-value sheets can be explained in terms of an improper yield function. Recent FLC calculations by Mellor,[27,35] Neale and Chater,[7] and Bassani *et al.*[8] indicate that the forming limit strains of a low R-value sheet are considerably reduced if the nonquadratic Hill or the Bassani yield function is used in place of the quadratic Hill yield function. The reductions occur when the stress exponents in the yield functions are less than 2 such that the resulting sharp curvatures at or near the equi-biaxial tension region easily lead to the plane strain condition for localized necking. A comparison of the quadratic and the nonquadratic Hill yield functions is illustrated in Figure 1. It is also worthy to note that the nonquadratic Hill yield behavior has been observed in 2024-aluminum with an R-value of 0.6.[36]

In a similar way, the inclusion of a J_3 term in the Drucker yield function also results in a sharper curvature near the equi-biaxial tension. The increased curvature is achieved, however, not by extending the yield surface in the $\sigma_1 = \sigma_2$ direction as in the nonquadratic Hill and the Bassani yield functions, but by reducing stress path hardening as represented by the reductions in the σ_1/σ_y ratios at and near the stress state of $\sigma_2/\sigma_1 = 0.5$ (the plane strain condition for $R = 1$) such that the plastic strain increment vector which lies normal to the yield surface can rotate to the plane strain condition more rapidly during plastic straining (see Figure 1(b)). As shown in Figure 1, the Drucker yield surface exhibits a rather extended region at which the plane strain condition is approximately satisfied. The consequence is that localized necking of sheets under equi-biaxial tension is predicted to occur at lower limit strains than that based on the quadratic Hill's yield function and, more importantly, the predicted FLC results are in good agreement with the experimental data of steels (see Figure 8 and Figure 9).

Experimental support for the use of Drucker's yield function for steels can be found in a recent study by Chan, Lindholm, and Wise[19] which shows that by a proper experimental determination of the C-value, the Drucker's yield function describes well the biaxial yield surfaces including normality and the plastic strain ratios of HY80 steel and that these yield surfaces are practically identical to the Bishop-Hill $\{110\}\langle 1\bar{1}1\rangle$ yield locus calculated by Bassani[18] for isotropic bcc metals. The C-value was determined to be 1.75 for HY80 steel. Comparing the pencile-glide yield surface to the $\{110\}\langle 1\bar{1}1\rangle$ Bishop-Hill yield surface, Chan *et al.* also noted that the shape of the yield locus would vary with the crystallography of slip and in particular depends on whether deformation occurs by pencile-glide or $\{110\}\langle 1\bar{1}1\rangle$ slip.[26] Recalling that upon a proper choice of the C-value, the Drucker yield function can represent both the pencile-glide and the Bishop-Hill $\{110\}\langle 1\bar{1}1\rangle$ yield surfaces, it seems logically that the C-value would also vary with the crystallography of slip and affect the FLC calculation through its influence on the shape of the yield locus. The present FLC calculation is based on a C-value of 2.25. A reduction in the C-value would increase the limit strain in the biaxial region ($\varepsilon_2 > 0$) because of a reduction in the sharpness of the yield surface curvature. It should also be noted that the Drucker yield function is applicable for isotropic materials only. In principle, it could be extended to anisotropic materials; the general form of the yield function and the associated flow laws remain to be developed, however.

According to Storen and Rice,[9] the use of deformation theory of plasticity in localized necking analysis can be rationalized on the basis that the yield surface develops a pointed vertex during plastic straining. At the vertex the incremental plastic strain vector is free to be directed anywhere between the two outward normals; the result is that the plane strain condition ($d\varepsilon_2 = 0$) required for the onset of localized necking can be readily attained. The formation of such a vertex on the yield surface would explain the FLC overpredictions in the $\varepsilon_2 > 0$ regime by the flow theory, and the reasonably good predictions by the deformation theory, for the low R-value ($R < 1$) sheets under biaxial straining (see Figures 3, 4, and 5). However, it should also be noted that even though yield vertex formation has been observed experimentally in certain cases[37] and shown to be a natural consequence of simultaneous slip on multiple slip systems,[38,39] the question of whether yield vertices develop during plastic straining is still a controversial one. In most cases, the pertinent yield surface and incremental plastic strain vector data required for resolving the issue are generally not available at immediate or large strain. Such are the cases for many of the aluminum and HSLA steel sheet alloys considered here (*e.g.*, 2036-T4 aluminum). The work-hardening rate of 2036-T4 aluminum has been found to vary with the stress state,[40] but the yield surface has been shown to change with plastic strain by inferring from plane strain tensile test data.[41] The incremental plastic strain vectors, however, were not measured as a function of stress state; it is thus not possible to determine whether or not a yield vertex develops during plastic straining nor is it possible to determine the shape of the yield surface in the biaxial tension region.

The available experimental data[41] also suggest that 2036-T4 aluminum might not work-harden isotropically as assumed. Recent theoretical computations reveal that FLCs obtained on the basis of kinematic or anisotropic hardening

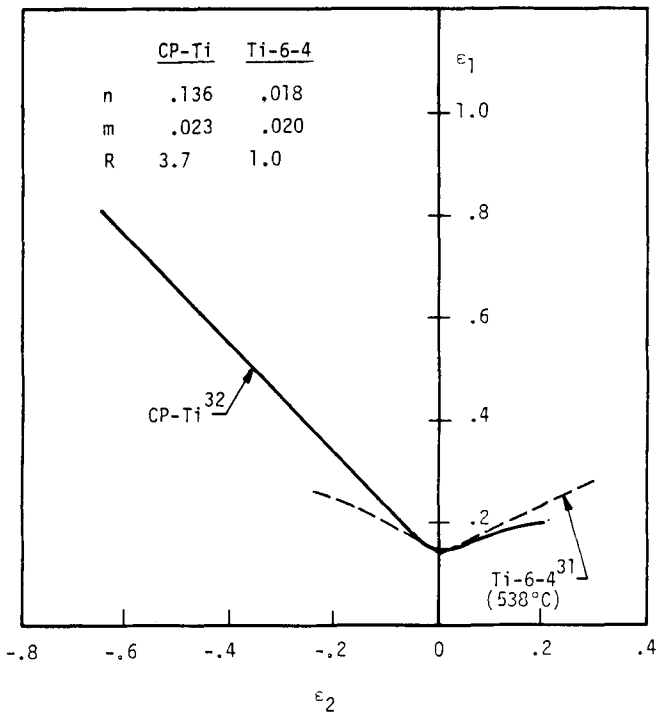

Fig. 10—A comparison of the FLCs of a moderately high R-value CP-Ti and a weak-textured, low R-value Ti-6Al-4V.

models generally differ from those calculated by assuming isotropic hardening and in certain cases yield better agreement with experimental results.[42,43] Thus, it appears that the stretchability behavior of the low R-value sheets ($R < 1$) can be rationalized on the basis of the vertex theory, but it is not the only rationale. Other possible rationales include anisotropic hardening[41,42] and smooth yield surfaces containing a sharp curvature in the biaxial tension region.[8,44] The mechanism responsible for the stretchability behavior observed in the low R-value sheets remains to be verified experimentally and might vary among the sheet alloys.

Figure 8 also indicates that the limit strain at the strain state of plane strain ($\varepsilon_2 = 0$) is independent of the yield function or the plasticity theory. At plane strain, the strain ratio within the imperfection is identical to that outside the imperfection ($\rho_A = \rho_B = 0$). Under these conditions, $\sigma_{1A}/\bar{\sigma}_A$ is equal to $\sigma_{1B}/\bar{\sigma}_B$ and Eq. [11] is reduced to be a function of n, m, f, the effective strains and their increments. As a result, the limit strains depend only on the n, m, and f values but not the yield function or the plasticity theory.[7] It is thus apparent that the influence of the yield function and the plasticity theory on the limit strain is important only for biaxial stretching involving positive minor strain ($\varepsilon_2 > 0$).

The question of whether a low R-value improves the biaxial stretchability of sheet metals still remains. Figure 10 compares the FLC of CP-Ti with that of a low R-value Ti-6Al-4V sheet.[31] In the $\varepsilon_2 > 0$ region, the forming limit strains of the Ti-6-4 sheet ($n = 0.018$, $m = 0.020$, $R = 1.0$) are expected to be smaller than that of CP Ti ($n = 0.14$, $m = 0.023$, $R = 3.7$) on the basis of lower n and m values. The Ti-6-4 FLC curve, however, lies above the CP-Ti curve, indicating superior forming limit strains. It thus led the author to conclude that the lower R-value of the Ti-6-4 sheet is responsible for the increase in the forming limit strains observed in the $\varepsilon_2 > 0$ regime, and the enhancement is likely the consequence of the less sharp curvature of the initial yield surface. In contrast, it has been shown previously that ε_1^* increases with the R-value in the $\varepsilon_2 < 0$ region but is independent of the R-value at plane strain ($\varepsilon_2 = 0$). According to Chan, Koss, and Ghosh,[5] this can be rationalized on the basis of increasing difficulties of attaining a critical thickness strain for localized necking at a higher R-value. These strain-state dependent effects of the R-value are generally observed in Figure 10. The influence of the R-value, however, appears to be more pronounced in the $\varepsilon_2 < 0$ than in the $\varepsilon_2 > 0$ region.

It should also be noted that the R-value can affect FLCs through its influence on fracture, as evidenced in Figure 7. Figure 8 shows that the FLC calculated using the Drucker yield function is quantitatively similar to Ghosh's fracture modified FLC,[2] especially at and near equi-biaxial tension. Hence, the present result raises the possibility that localized necking and fracture might occur at approximately the same limit strain in A-K steel.

V. CONCLUSIONS

1. The FLCs calculated on the basis of the Marciniak-Kuczynski analysis are sensitive to the choices of yield function and plasticity theory when $\varepsilon_2 > 0$. None of the yield functions nor the plasticity theories examined can predict with confidence the stretchability of a variety of sheet alloys in the $\varepsilon_2 > 0$ regime.
2. When used in conjunction with the quadratic Hill yield function, the flow theory gives good FLC predictions for sheets with high R-value ($R \geq 3.7$) while the deformation theory yields good FLC predictions for sheets with low R-values ($R < 1$).
3. The effects of plastic anisotropy on the biaxial stretchability of thin sheets appear to be mixed and strain-state dependent. The forming limit strains are enhanced by a low R-value in the $\varepsilon_2 > 0$ region of an FLC but increase with the R-value in the $\varepsilon_2 < 0$ region and are independent of the R-value at plane strain ($\varepsilon_2 = 0$).
4. The enhancement of ε_1^* by a high R-value in $\varepsilon_2 < 0$ region is the result of increasing difficulties in attaining a critical thickness strain. The increase of ε_1^* with decreasing R-values in the $\varepsilon_2 > 0$ region is the consequence of a less sharp curvature in the initial yield surface.

APPENDIX I

The quadratic Hill yield function, f', for plane stress and the associated flow laws are obtained from Reference 15.

$$f' = (G + H)\sigma_1^2 - 2H\sigma_1\sigma_2 + (F + H)\sigma_2^2 = 1 \quad [A1]$$

$$d\varepsilon_1 = d\lambda[H(\sigma_1 - \sigma_2) + G\sigma_1]$$

$$d\varepsilon_2 = d\lambda[F\sigma_2 + H(\sigma_2 - \sigma_1)] \quad [A2]$$

$$d\varepsilon_3 = d\lambda[-G\sigma_1 - F\sigma_2]$$

where F, G, and H are anisotropy coefficients, and $d\lambda$ is a deformation-history-dependent parameter. According to

Hill, the appropriate effective stress and the incremental effective plastic strain would be

$$\bar{\sigma} = \sqrt{\frac{3}{2}}\left[\frac{(G + H)\sigma_1^2 - 2H\sigma_1\sigma_2 + (F + G)\sigma_2^2}{F + G + H}\right]^{1/2} \quad [A3]$$

$$d\bar{\varepsilon} = \sqrt{\frac{2}{3}}\frac{(F + G + H)^{1/2}}{Q}[F(Gd\varepsilon_2 - Hd\varepsilon_3)^2 + G(Hd\varepsilon_3 - Fd\varepsilon_1)^2 + H(Fd\varepsilon_1 - Gd\varepsilon_2)^2]^{1/2} \quad [A4]$$

where

$$Q = FG + GH + HF$$

For material exhibiting normal anisotropy, F, G, and H are related to the R-value which is the ratio of the width strain to thickness strain in a uniaxial tensile test.

$$\frac{H}{F} = \frac{H}{G} = R \quad [A5]$$

and

$$F = G \neq H$$

Equations [A3], [A4], and [A2] can be expressed in terms of the R-value through Eq. [A5]. The resulting equations are shown in Eqs. [2], [3], and [4], respectively. For uniaxial tension, Eqs. [2] and [3a] can be reduced to give the following relationship:

$$\bar{\sigma} = \sqrt{\frac{3}{2}}\sqrt{\frac{1 + R}{2 + R}}\sigma_1$$

$$d\bar{\varepsilon} = \sqrt{\frac{2}{3}}\sqrt{\frac{2 + R}{1 + R}}d\varepsilon_1 \quad [A6]$$

and

$$\bar{\sigma}d\bar{\varepsilon} = \sigma_1 d\varepsilon_1$$

Therefore, the effective stress and the incremental effective plastic strain are related to σ_1 and $d\varepsilon_1$ on the basis of equivalent plastic work.

The associated flow laws for the Drucker yield function (Eq. [6]) can be obtained on the basis of the incremental (flow) theory of plasticity.

$$d\varepsilon_{ij} = d\lambda\frac{\partial g}{\partial \sigma_{ij}} \quad [A7]$$

Using Eq. [A7], the incremental plastic strains in the 1 and 2 principal directions are derived as follows:

$$d\varepsilon_1 = Zd\lambda[9(2\sigma_1 - \sigma_2)J_2^2 - 2C(2\sigma_1^2 - 2\sigma_1\sigma_2 - \sigma_2^2)J_3] \quad [A8]$$

$$d\varepsilon_2 = Zd\lambda[9(2\sigma_2 - \sigma_1)J_2^2 - 2C(2\sigma_2^2 - 2\sigma_1\sigma_2 - \sigma_1^2)J_3] \quad [A9]$$

where

$$Z = \frac{3}{27 - 4C}$$

The plastic strain ratio, ρ, is readily obtained by dividing Eq. [A9] by Eq. [A8] to give the expression shown in Eq. [8]. Assuming constancy of volume during plastic deformation, the incremental thickness strain can be written in terms of ρ and $d\varepsilon_1$ by substituting Eq. [3c] into Eq. [9]

$$d\varepsilon_3 = -(1 + \rho)d\varepsilon_1 \quad [A10]$$

APPENDIX II

(i) *M-K analysis using the quadratic Hill yield function and the flow theory of plasticity.*

Eq. [11] can be rearranged to yield the following form:

$$\frac{(\sigma_{1A}/\bar{\sigma}_A)X^m}{(\sigma_{1B}/\sigma_B)} = fT^{-n}\exp[\varepsilon_{3B} - \varepsilon_{3A}] \quad [A11]$$

where

$$X = d\bar{\varepsilon}_A/d\bar{\varepsilon}_B, \qquad T = \frac{\bar{\varepsilon}_A}{\bar{\varepsilon}_B}$$

From the associated flow laws in Eq. [4], we obtain

$$\frac{d\varepsilon_1}{\left(\frac{1 + R}{R}\right)\sigma_{1A} - \sigma_{2A}} = \frac{3R\,d\bar{\varepsilon}_A}{2(2 + R)\bar{\sigma}_A} \quad [A12]$$

After substituting Eq. [3a] and rearranging terms, $\sigma_{1A}/\bar{\sigma}_A$ has been found to be

$$\frac{\sigma_{1A}}{\bar{\sigma}_A} = q\sqrt{1 - B'} \quad [A13]$$

where

$$q = \sqrt{\frac{2}{3}}\sqrt{\frac{(2 + R)(1 + R)}{1 + 2R}}$$

$$B' = \frac{(1 + 2R)\rho^2}{(1 + R)^2\left(1 + \frac{2R}{1 + R}\rho + \rho^2\right)} \quad [A14]$$

Following the procedures of Marciniak *et al.*,[16] $\sigma_{1B}/\bar{\sigma}_B$ is given by the following expression:

$$\frac{\sigma_{1B}}{\bar{\sigma}_B} = q[1 - B'X^2]^{1/2} \quad [A15]$$

Using Eqs. [3a] and [A10], ε_{3A} is expressed in terms of ρ_A and $\bar{\varepsilon}_A$ to give

$$\varepsilon_{3A} = -C\bar{\varepsilon}_A$$

where

$$C = \frac{1 + \rho_A}{q\sqrt{1 + \left(\frac{2R}{1 + R}\right)\rho_A + \rho_A^2}} \quad [A16]$$

Eqs. [A13], [A15], and [A16] are then substituted into Eq. [A11], yielding

$$\frac{\sqrt{1 - B'}X^m}{\sqrt{1 - B'X^2}} = fT^{-n}\exp[\varepsilon_{3B} + C\bar{\varepsilon}_A] \quad [A17]$$

Following the lengthy mathematical procedures outlined in

Reference 16, which involve both the flow laws (Eq. [4]) and the constraint equation (Eq. [12]), the thickness strain within the imperfection can be expressed in terms of $d\bar{\varepsilon}_A$ and $d\bar{\varepsilon}_B$ as follows:

$$d\varepsilon_{3B} = -\{A'[1 - B'X^2]^{1/2} + DX\}d\bar{\varepsilon}_B \quad [A18]$$

where

$$A' = \sqrt{\frac{3}{2}}\sqrt{\frac{1 + 2R}{(2 + R)(1 + R)}} \quad [A19]$$

$$D = \frac{A\rho_A}{(1 + R)\sqrt{1 + \left(\frac{2R}{1 + R}\right)\rho_A + \rho_A^2}} \quad [A20]$$

and B' is given by Eq. [A14]. For a given ρ_A, $d\bar{\varepsilon}_B$($d\bar{\varepsilon}_B$ is prescribed) and $\bar{\varepsilon}_B$, Eqs. [17] and [A18] can be solved simultaneously using the 4th order Runge-Kutta method to obtain $d\bar{\varepsilon}_A$. $\bar{\varepsilon}_A$ and $\bar{\varepsilon}_B$ are then updated by adding $d\bar{\varepsilon}_A$ and $d\bar{\varepsilon}_B$ to their previous values, respectively. The incremental solution procedure is repeated until $d\bar{\varepsilon}_A$ is less than 1×10^{-4}.

(ii) *M-K analysis using the quadratic Hill yield function and the deformation theory of plasticity.*

Eq. [11] remains valid when the deformation theory is used in the M-K analysis instead of the flow theory. Following the procedures outlined in Section (i) but replacing the flows with the deformation laws, Eq. [A17] becomes

$$\frac{\sqrt{1 - B'X^m}}{\sqrt{1 - B'T^2}} = fT^{-n}\exp[\varepsilon_{3B} + C\bar{\varepsilon}_A] \quad [A21]$$

B' and C are given by Eqs. [A14] and [A16], respectively. On the other hand, Eq. [12] is replaced by

$$\varepsilon_{2A} = \varepsilon_{2B}$$

and Eq. [A18] becomes

$$\varepsilon_{3B} = -P\bar{\varepsilon}_B \quad [A22]$$

where

$$P = A'[1 - B'T^2]^{1/2} + DT$$

A' and D are shown in Eqs. [A19] and [A20], respectively. Eq. [A22] is then substituted into Eq. [A21] to give the following expression:

$$\frac{\sqrt{1 - B'X^m}}{\sqrt{1 - B'T^2}} = fT^{-n}\exp[C\bar{\varepsilon}_A - P\bar{\varepsilon}_B] \quad [A23]$$

Eq. [A23] is reduced to Eq. [9] of Reference 10 when $R = 1$. For a given ρ_A, $d\bar{\varepsilon}_B$ ($d\bar{\varepsilon}_B$ is prescribed), $\bar{\varepsilon}_A$ and $\bar{\varepsilon}_B$, Eq. [A23] can be solved using a simple Newton-Raphson method to obtain $d\bar{\varepsilon}_A$. At each incremental step, $\bar{\varepsilon}_A$ and $\bar{\varepsilon}_B$ are updated by adding $d\bar{\varepsilon}_A$ and $d\bar{\varepsilon}_B$, respectively. The incremental procedure is repeated until $d\bar{\varepsilon}_A$ is less than 1×10^{-4}.

(iii) *M-K analysis using the Drucker yield functions and the flow theory of plasticity*

The $\sigma_{1A}/\bar{\sigma}_A$ and $\sigma_{1B}/\bar{\sigma}_B$ quantities in Eq. [11] are obtained from Eq. [7] by replacing α with α_A and α_B, respectively. The thickness strain ε_{3A} is obtained using Eq. [A10] and Eq. [3A] by substituting $R = 1$ and the plastic strain ratio, ρ_A

$$\varepsilon_{3A} = -\frac{(1 + \rho_A)}{C_1}\bar{\varepsilon}_A \quad [A24]$$

where

$$C_1 = \frac{2}{\sqrt{3}}(1 + \rho_A + \rho_A^2)^{1/2}$$

Similarly, ε_{3B} is obtained as

$$\varepsilon_{3B} = \frac{-(1 + \rho_B)\bar{\varepsilon}_B}{C_2} \quad [A25]$$

with

$$C_2 = \frac{2}{\sqrt{3}}(1 + \rho_B + \rho_B^2)^{1/2}$$

After substituting the expressions for $\sigma_{1A}/\bar{\sigma}_A$, $\sigma_{1B}/\bar{\sigma}_B$, ε_{3A} and ε_{3B}, Eq. [11] is expressed in terms of α_A, α_B, ρ_A, ρ_B, $\bar{\varepsilon}_A$, $\bar{\varepsilon}_B$, $d\bar{\varepsilon}_A$, $d\bar{\varepsilon}_B$, and other material constants. Eq. [12] is also expressed in terms of $d\bar{\varepsilon}_A$ and $d\bar{\varepsilon}_B$ as follows:

$$\frac{\rho_A}{C_1}d\bar{\varepsilon}_A = \frac{\rho_B}{C_2}d\bar{\varepsilon}_B \quad [A26]$$

For a given α_A, ρ_A is calculated using Eq. [8]. Substituting the prescribed values of α_A, ρ_A, $d\bar{\varepsilon}_B$, and the current values of $\bar{\varepsilon}_A$ and $d\bar{\varepsilon}_B$, $d\bar{\varepsilon}_A$ and α_B (ρ_B is calculated in terms of α_B using Eq. [8]) are obtained by solving Eqs. [11] and [A26] simultaneously using the Newton-Raphson method. $\bar{\varepsilon}_A$ and $\bar{\varepsilon}_B$ are updated at each solution step by adding $d\bar{\varepsilon}_A$ and $d\bar{\varepsilon}_B$, respectively. The incremental procedure is repeated until $d\bar{\varepsilon}_A$ is less than 1×10^{-4}. It should be noted that this incremental solution procedure is a very general one; it is not restricted to a particular yield function and avoids the lengthy mathematical manipulations associated with the procedures described in Section (i).

ACKNOWLEDGMENTS

The author wishes to thank Professor D. A. Koss and Dr. U. S. Lindholm for many stimulating discussions and valuable suggestions. This work was initiated at Michigan Technological University and supported by the Office of Naval Research through Contract No. N00014-76-C-0037, NR031-756. The work was finished under the Internal Research Program of Southwest Research Institute.

REFERENCES

1. S. S. Hecker: *Formability, Analysis, Modeling, and Experimentation*, S. S. Hecker, A. K. Ghosh, and H. L. Gegel, eds., TMS-AIME, Warrendale, PA, 1978, p. 150.
2. A. K. Ghosh: *Mechanics of Sheet Metal Forming*, D. P. Koistinen and N. M. Wang, eds., Plenum Press, New York, NY, 1978, p. 287.
3. K. S. Chan and D. A. Koss: *Metall. Trans. A*, 1983, vol. 14A, p. 1333.
4. K. S. Chan and D. A. Koss: *Metall. Trans. A*, 1983, vol. 14A, p. 1343.
5. K. S. Chan, D. A. Koss, and A. K. Ghosh: *Metall. Trans. A*, 1984, vol. 15A, p. 323.
6. R. Hill: *J. Mech. Phys. Solids*, 1952, vol. 1, p. 19.
7. K. W. Neale and E. Chater: *Int. J. Mech. Sci.*, 1980, vol. 22, p. 563.
8. J. L. Bassani, J. W. Hutchinson, and K. W. Neale: in *Metal Forming Plasticity Symposium*, H. Lippman, ed., Springer-Verlag, Berlin, 1979, p. 1.

9. S. Storen and J. R. Rice: *J. Mech. Phys. Solids*, 1975, vol. 23, p. 421.
10. J. W. Hutchinson and K. W. Neale: *Mechanics of Sheet Metal Forming*, D. P. Koistinen and N. M. Wang, eds., Plenum Press, New York, NY, 1978, p. 127, p. 269.
11. J. Christoffersen and J. W. Hutchinson: *J. Mech. Phys. Solids*, 1979, vol. 27, p. 465.
12. Z. Marciniak and K. Kuczynski: *Int. J. Mech. Sci.*, 1967, vol. 9, p. 609.
13. A. Needlemen and N. Triantafyllidis: *Trans. ASME*, 1978, vol. 110, p. 164.
14. R. Sowerby and J. L. Duncan: *Int. J. Mech. Sci.*, 1971, vol. 13, p. 217.
15. R. Hill: *The Mathematical Theory of Plasticity*, Chapter XII, Oxford Univ. Press, London, 1967, p. 320, p. 334.
16. Z. Marciniak, K. Kuczynski, and T. Pokora: *Int. J. Mech. Sci.*, 1973, vol. 15, p. 780.
17. R. Hill: *Math. Proc. Cambridge Phil. Soc.*, 1979, vol. 85, p. 179.
18. J. L. Bassani: *Int. J. Mech. Sci.*, 1977, vol. 19, p. 651.
19. K. S. Chan and U. S. Lindholm: Southwest Research Institute, San Antonio, TX 78284; J. Wise, David Taylor Naval Ship R&D Center, Norfolk Naval Shipyard, Portsmouth, VA 23709, unpublished research, 1984.
20. D. C. Drucker: *J. App. Mech., Trans. ASME*, 1949, vol. 16, p. 349.
21. D. Lee and F. Zaverl: *Int. J. Mech. Sci.*, 1982, vol. 24, p. 157.
22. J. Thomas, S. I. Oh, and H. L. Gegel: in *Advanced Processing Methods for Titanium*, TMS-AIME, Warrendale, PA, 1980, p. 863.
23. H. W. Swift: *J. Mech. Phys. Solids*, 1952, vol. 1, p. 1.
24. W. A. Backofen: *Deformation Processing*, Addison-Wesley, Reading, MA, 1972, p. 25, p. 80.
25. J. F. W. Bishop and R. Hill: *Phil. Mag.*, 1951, vol. 42, p. 441, p. 1298.
26. K. S. Chan, U. S. Lindholm, and J. Wise: *Metall. Trans. A*, 1984, vol. 15A, p. 2097.
27. P. B. Mellor and A. Parmar: *Mechanics of Sheet Metal Forming*, D. P. Koistinen and N. M. Wang, eds., Plenum Press, New York, NY, 1978, p. 53.
28. A. K. Ghosh and S. S. Hecker: *Metall. Trans.*, 1974, vol. 5, p. 2161.
29. R. Sowerby and B. K. Sareen: ASTM STP 647, B. A. Niemeier, A. K. Schmieder, and J. R. Newby, eds., ASTM, 1987, p. 49.
30. A. K. Ghosh: *Metals Engineering Quarterly*, August 1975, vol. 15, p. 53.
31. K. Okazaki, M. Kagawa, and H. Conrad: in *Titanium '80*, H. Kimura and O. Izumi, eds., TMS-AIME, Warrendale, PA, 1980, p. 863. See also J. F. Thomas, S. I. Oh, and H. L. Gegel: In *Advance Processing Methods for Titanium*, TMS-AIME, Warrendale, PA, 1982, p. 81.
32. R. J. Bourcier: M.S. Thesis, Michigan Technological University, Houghton, MI, 1981.
33. S. S. Hecker: *Sheet Metal Industries*, November 1975, vol. 52, p. 671.
34. C. W. Lentz, D. A. Koss, M. G. Stout, and S. S. Hecker: *Metall. Trans. A*, 1983, vol. 14A, p. 2527.
35. P. B. Mellor: *Int. Met. Rev.*, 1981, vol. 26, p. 1.
36. M. G. Stout, S. S. Hecker, and R. Bourcier: *J. Eng. Mat. Tech.*, Trans. ASME, 1983, vol. 105, no. 4, p. 242.
37. S. S. Hecker: *Constitutive Equations in Viscoplasticity: Computational and Engineering Aspects*, J. A. Stricklin and K. J. Saczakski, eds., ASTM, 1976, p. 1.
38. J. F. W. Bishop: *Phil. Mag.*, 1953, vol. 44, p. 51.
39. R. Hill: *J. Mech. Phys. Solids*, 1967, vol. 15, p. 79.
40. J. V. Laukonis and A. K. Ghosh: *Metall. Trans. A*, 1978, vol. 9A, p. 1849.
41. R. H. Wagoner: *Metall. Trans. A*, 1980, vol. 11A, p. 165.
42. V. Tvergaard: *Int. J. Mech. Sci.*, 1978, vol. 20, p. 651.
43. C. C. Chu: *J. Mech. Phys. Solids*, 1984, vol. 32, p. 197.
44. S. N. Rasmussen: *Int. J. Mech. Sci.*, 1982, vol. 24, p. 729.